Anomalous thermal transport and strong violation of Wiedemann-Franz law in the critical regime of a charge density wave transition

Erik D. Kountz, Jiecheng Zhang, Joshua A. W. Straquadine, Anisha G. Singh, Maja D. Bachmann, Ian R. Fisher, Steven A. Kivelson, and Aharon Kapitulnik

Phys. Rev. B **104**, L241109 — Published 22 December 2021

DOI: 10.1103/PhysRevB.104.L241109

Anomalous thermal transport and strong violation of Wiedemann-Franz law in the critical regime of a charge density wave transition

Erik D. Kountz,[1,2,3] Jiecheng Zhang,[1,2,3] Joshua A. W. Straquadine,[1,2,4] Anisha G. Singh,[1,2,4] Maja D. Bachmann,[1,2,4] Ian R. Fisher,[1,2,4] Steven A. Kivelson,[1,2,3] and Aharon Kapitulnik[1,2,3,4]

[1] *Stanford Institute for Materials and Energy Sciences, SLAC National Accelerator Laboratory, 2575 Sand Hill Road, Menlo Park, CA 94025*
[2] *Geballe Laboratory for Advanced Materials, Stanford University, Stanford, CA 94305*
[3] *Department of Physics, Stanford University, Stanford, CA 94305*
[4] *Department of Applied Physics, Stanford University, Stanford, CA 94305*

(Dated: December 8, 2021)

$ErTe_3$ is a model system used to explore thermal transport in a layered charge density wave (CDW) material. We present thermal diffusivity, resistivity, and specific heat data: There is a sharp decrease in thermal conductivity parallel and perpendicular to the primary CDW at the CDW transition temperature. Yet, the resistivity changes more gradually. Using the Wiedemann Franz law, well above and below T_c a consistent description of the thermal transport applies with essentially independent electron and phonon contributions. In the critical regime no such description is possible; the observed behavior corresponds to a strongly coupled electron-phonon critical 'soup.'

Unlike the standard paradigm [1, 2], in more than one spatial dimension, due to imperfect nesting, charge density wave (CDW) order (unlike superconducting order) only emerges for interactions greater than a critical strength. Generically, the "mechanism" involves strong electron-electron and electron-phonon interactions. Strong-coupling is particularly reflected in large ratios of the induced gap to T_c. For the material in this study, $ErTe_3$, the gap associated with the primary CDW transition at $T_{CDW1} \approx 265$ K is $\Delta_1 \approx 175$ meV, implying $2\Delta_1/k_B T_{CDW1} \approx 15$ [3, 4]. Since weakly interacting quasiparticles and well defined phonons give good account of the physics at $T > T_{CDW1}$ and at low temperatures deep in the ordered phase, it is conventional (following classical critical phenomena in metals) to adopt a phenomenological approach where low energy quasiparticles and the bulk of phonons are weakly coupled to "critical modes" associated directly with the CDW transition. Our results challenge this standard perspective.

Electrical and thermal transport measurements provide important information about electronic structure and scattering processes in complex quantum materials. When transport is dominated by weakly interacting (emergent) elementary excitations, thermal conductivity can be expressed as the sum of electronic and phononic contributions, $\kappa \approx \kappa_{el} + \kappa_{ph}$. Furthermore, for quasi-elastic scattering processes κ_{el} is related to electrical conductivity by the Wiedemann-Franz (WF) law, i.e. $\kappa_{el}/\sigma = L_0 T$, where $L_0 = \pi^2 k_B^2/3e^2 \approx 2.44 \times 10^{-8} \mathrm{W\Omega K^{-2}}$ is a universal constant. Observing this ratio indicates "standard" transport in a given electronic system, while significant violations of the WF law may indicate a breakdown of the quasiparticle description.

In this letter we examine electrical and thermal transport in the layered material $ErTe_3$, which exhibits CDW transitions at $T_{CDW1} \approx 265$ K and $T_{CDW2} \approx 160$ K. Here T_{CDW1} marks the onset of a "primary" CDW order with c-direction ordering vector q_{CDW1}. Below T_{CDW2} a "secondary" orthogonal a-direction CDW component q_{CDW2} appears (a and c are in-plane lattice parameters). Despite the nearly tetragonal crystal lattice ($a \sim c$ with b perpendicular), the phase at $T_{CDW1} > T > T_{CDW2}$ has unidirectional CDW order, while the low temperature CDW is bidirectional with inequivalent amplitudes in the directions. $ErTe_3$ is an ideal "model system" because it is stoichiometric and can be synthesized with a high degree of crystalline perfection and little disorder (very low residual resistivity - $\rho(T) < 1$ $\mu\Omega$-cm at low T and resolution limited Bragg peaks associated with the CDW order). It boasts broad metallic bands with plasma frequency between 2.5 eV [3] and 5.8 eV [5] in the CDW state. Moreover, disorder can be explored systematically by Pd intercalation [6–8].

Our primary result is that thermal transport in a critical regime below T_{CDW1} appears inconsistent with quasiparticle transport. Assuming κ_{el} that satisfies the WF law, separate from κ_{ph}, one is forced to infer an unphysically large depression in lattice thermal transport. This demonstrative evidence for breakdown of the WF law and quasiparticle concept is strongly asymmetric, extending farther below T_{CDW1} than above it. In addition, we also observe: *i*) Similar to other strongly interacting CDW systems, large anomalies are observed in the temperature derivative of the resistivity and reflectivity (Fig. 2(b)), which, assuming that Fisher-Langer theory [9] applies, stands in sharp contrast to the small heat capacity anomaly[10]. *ii*) The behavior of various linear response tensors near criticality (Figs. 1(b) and 2(a)) depends strongly on direction. As T decreases, the a-direction resistivity, ρ^a, has a pronounced critical singularity at T_{CDW1} followed by a broad maximum and subsequent low temperatures drop, as previously discussed [11]. Conversely, the critical anomaly in ρ^c at T_{CDW1} is much weaker, and neither component shows any clear

non-analyticity at T_{CDW2}. In contrast, the thermal diffusivity has a large sharp decrease at T_{CDW1} along both the a- and c- directions, followed by a faster recovery along the c-direction. Also evident from Fig. 2(a), the thermal diffusivity more closely resembles the temperature derivative of the resistivity. *iii*) Thermal diffusivity in both directions increases markedly below T_{CDW2}, which through suppression of this effect by weak Pd-intercalation are argued to be electronic in origin (Fig. 3).

$ErTe_3$ samples were grown using a Te self-flux technique, ensuring melt purity, and producing large crystals with a high degree of structural order [12]. Being air sensitive, $ErTe_3$ must be stored in an oxygen and moisture-free environment. Crystal orientation was determined with XRD. Thermal diffusivity and differential reflectivity (dR/dT) were measured using a photothermal microscope [13]. Details of specific heat, resistivity, and thermal diffusivity measurements are described in the Supplementary Material (SM): [14]. Figure 1(a)

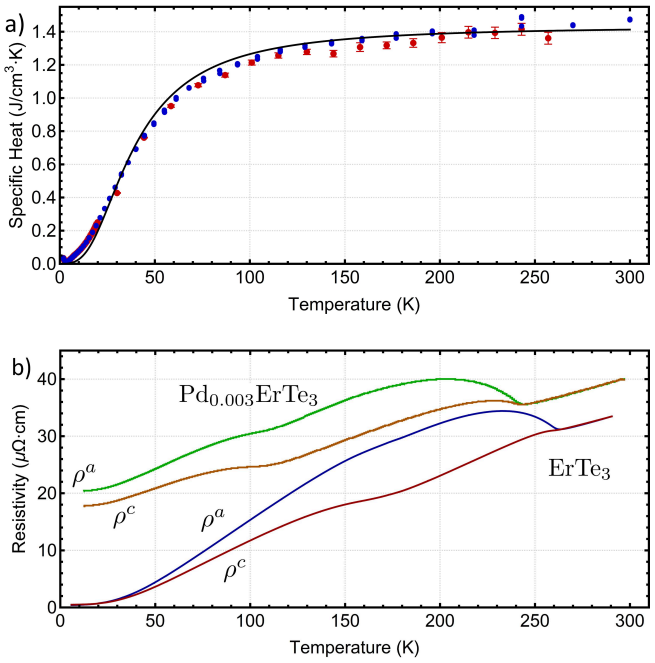

FIG. 1. (a) Specific heat of two $ErTe_3$ crystals. Solid line is a Debye model fit ($\theta_D = 160$ K). CDW transitions at $T_{CDW1} \approx 265$ K and $T_{CDW2} \approx 160$ K produce no prominent critical signatures. (b) Resistivity of similar crystals (blue: a axis, red: c axis) and of 0.3% Pd-intercalated crystal (green: a axis, orange: c axis). Note the decrease in the CDW transitions and increased residual resistivity for the intercalated sample.

shows specific heat of two $ErTe_3$ crystals over a wide temperature range. The data closely follow the Debye approximation with $\theta_D \approx 160$ K, including above and below both CDW transitions saturating at the high temperature Dulong-Petit value. Previous measurements of the specific heat anomaly at T_{CDW1} [10] find $\Delta c_p \approx 0.0144$ J/cm^3·K, below the resolution of the present measurements, and surprisingly of "normal magnitude" given the large value of $2\Delta_1/k_BT_{CDW1} \approx 15$ inferred from ARPES measurements[4]. By contrast, both CDW transitions produce large anomalies in the thermal diffusivity data on a same-batch crystal as shown in Fig. 2(a). Particularly, at T_{CDW1} diffusivity along both axes drops over a third from ~ 0.21 cm^2/s to ~ 0.14 cm^2/s.

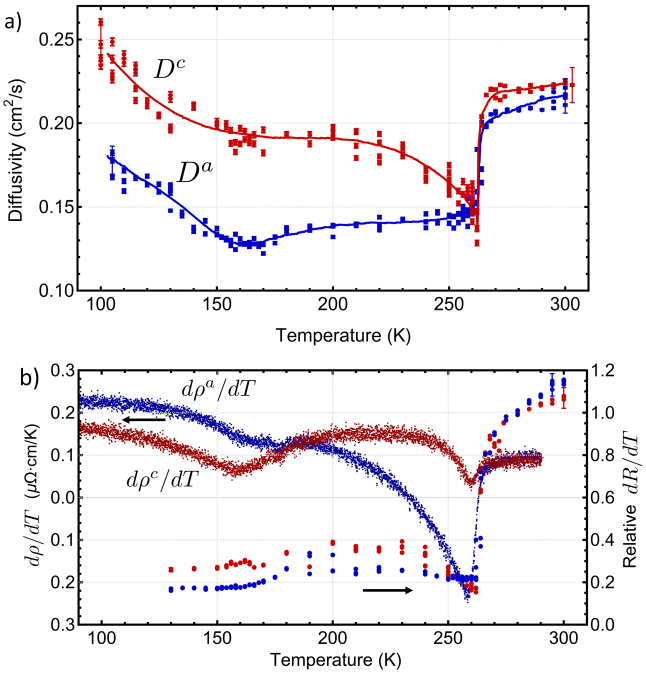

FIG. 2. (a) $ErTe_3$ thermal diffusivity measured using photothermal microscope showing CDW transitions at $T_{CDW1} \approx 265$ K and $T_{CDW2} \approx 160$ K. Scatter of data primarily associated with one-pixel control of measurement position and relative distance between heating and probing laser spots. Selected data near 100 K and 300 K show representative 5% systematic uncertainty, see SM [14]. Solid lines are guides to the eye. (b) Amplitude of temperature derivative of reflectivity - dR/dT normalized by this amplitude at $T_0 = 280$ K (full circles, right axis) vs. temperature. Temperature derivative of the resistivity, $d\rho/dT$, extracted from Fig. 1(b) (left axis) is shown for comparison. Blue: a axis, red: c axis. Selected data near 130 K and 300 K show representative 5% systematic uncertainty.

Figure 1(b) shows resistivity data on same-batch crystals (see SM: [14] for determination of geometrical factors [15]). The trend in the data is similar to previously measured RTe_3 crystals [16], particularly $ErTe_3$ [6, 15], featuring a strong anomaly along the a-axis (perpendicular to the primary CDW direction) at T_{CDW1} and only a weak wiggle along the c-axis near T_{CDW2}. In contrast, thermal diffusivity along both axes sharply decreases at T_{CDW1} and gradually increases below T_{CDW2} (Fig. 2(a)). However, these thermal diffusivity anomalies resemble more the features of the derivative of the resistivity $d\rho/dT$ as seen in Fig. 2(b). Similarly, the magni-

tude (see SM: [14]) of the temperature derivative of the reflectivity dR/dT at $h\nu \approx 1.5$ eV (820 nm wavelength) shows a large sharp decrease at T_{CDW1}, although here no anomaly is visible at T_{CDW2}.

Figure 3 demonstrates the effect of purposefully introduced weak disorder on the temperature dependence of thermal diffusivity. Focusing on the a-axis (no noticeable effects appear in the c-direction for this weak disorder [7]), we compare the diffusivity of $Pd_{0.003}ErTe_3$ to pure $ErTe_3$ (Fig. 2(a)). While T_{CDW1} is suppressed to 250 K, the sharp drop in diffusivity is not affected. However, below T_{CDW2} (here ~ 130 K) there is a striking intercalation induced difference; the pronounced upturn of the diffusivity in the pure material vanishes.

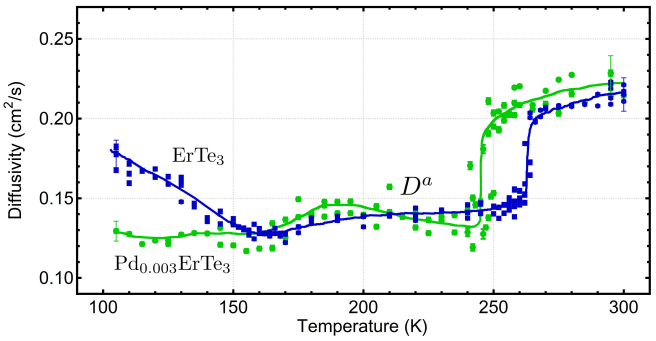

FIG. 3. Thermal diffusivity along a-axis of $ErTe_3$ (blue) and $Pd_{0.003}ErTe_3$ (green). Selected data near 100 K and 300 K show representative 5% systematic uncertainty, see SM: [14]. Solid lines to guide the eye.

$ErTe_3$ resistivity was measured before [15, 16] and the temperature dependence understood in terms of the material band structure [11]. Specifically, when the primary CDW forms along the c-axis, the resistivity start increasing along the perpendicular a-direction. Likewise, when the secondary CDW forms along the a-axis, there is a larger change in $d\rho/dT$ along the c-direction.

In a photothermal measurement we extract thermal transport information by analyzing the phase delay in change of reflectivity from a probed point on the sample surface due to a propagating heat wave originating from a point-like source modulated at frequency ω. The reflected light amplitude $R(\nu)$, (where $\nu = c/\lambda$ is the probing light frequency with wavelength λ) detected at the probing point is proportional to dR/dT. While within the heating spot temperature may rise a few degrees, taking the system out of equilibrium, this small amount of heat quickly dissipates out, not affecting the global temperature, while far from the heating spot guarantees very small δT and thus linear response (see [17, 18] and SM: [14]). Optical reflectivity was previously measured on $ErTe_3$ [3, 5] over the entire frequency range, exceeding the room-temperature plasma frequency, which depending on the global fit, is estimated between $20,000$ cm^{-1} (500 nm) [3] to $47,000$ cm^{-1} (213 nm) [5]. At our 820 nm probing wavelength, a Drude scattering rate $(1/\tau) \sim 20$ times smaller with a full Drude-Lorentz expression are needed to fit the experimental data in the whole frequency range [3, 5]. Since the range of interband transition described by a set of Lorentz harmonic oscillators is temperature independent, it is reasonable to assume much of the temperature-dependent component of the reduction in reflectivity comes from the temperature dependence of the relaxation time, which is strongly affected by scattering from CDW fluctuations [3]. We then assume $R(\nu) = R_0(\nu) + \Delta R(\nu\tau)$ (e.g., by extending the Hagen-Rubens relation to near-IR corresponding to our probing light, $R(\nu) \simeq 1 - 2\sqrt{\nu\rho}$, with ρ the Drude resistivity); thus $dR/dT \propto d\tau/dT$.

In a seminal work, Fisher and Langer [9] showed that the leading (perturbative) effect of scattering of conduction electrons by classical (i.e. approximately static) critical modes leads to $d\rho/dT \propto c_{CDW}$, where c_{CDW} is the specific heat associated with critical fluctuations near a finite T phase transition. Examining the temperature derivative of the resistivity, particularly the a-direction, indeed reveals what appears to be a broadened discontinuity at T_{CDW1}, similar to the behavior of the reflectivity. This mean-field-like form agrees with the shape of the anomaly observed in direct measurements of specific heat [10, 19], although the relative strength of the anomaly is much weaker in those measurements (essentially invisible in Fig. 1a). Despite similar behaviors at T_{CDW1}, at lower temperatures $d\rho/dT$ and dR/dT exhibit substantially different thermal evolutions. The former, but not the latter recovers rapidly to values comparable to the CDW transition[20]. Furthermore, near T_{CDW2}, $d\rho/dT$ shows a relatively weak but still clear critical anomaly, while the effect of the second CDW transition is difficult to discern in dR/dT.

More insight between electrical and thermal transport is obtained using their respective Einstein relations:

$$\sigma = \chi_{el} D_{el}; \qquad \kappa = c_p D_Q \tag{1}$$

with χ_{el} the electronic compressibility, c_p the total specific heat, D_{el} and D_Q the electronic and heat diffusivities respectively. While χ_{el} is a response function of only the electron system, the specific heat of the material, particularly at high temperatures, may be lattice dominated. A simple kinetic approach where electrons and phonons transport heat in parallel channels implies $\kappa = \kappa_{el} + \kappa_{ph} = c_{el} D_{el} + c_{ph} D_{ph}$, where c_{el} and c_{ph} are the electronic and lattice specific heats and D_{el} and D_{ph} are the respective diffusivities.

The total thermal conductivity along the a and c axes can be calculated following Eqn. 1 and using the measured specific heat and thermal diffusivity as is shown in Fig. 4 together with a best-fit guide to the eye curve. Assuming that WF law holds, we calculate the electronic thermal conductivity from the resistivity $\kappa_{el} =$

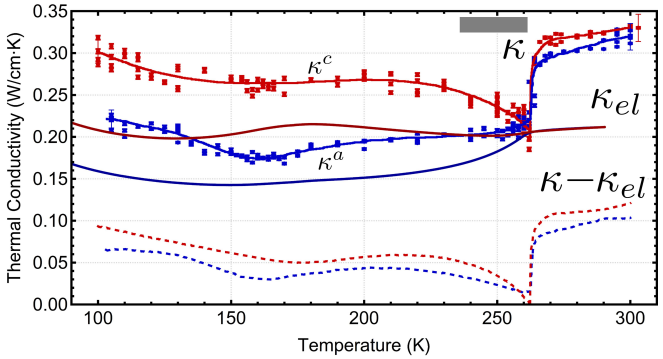

FIG. 4. Total thermal conductivity, κ (solid line through the data is guide to eye), electronic component κ_{el} computed from ρ assuming WF law (solid), and $\Delta\kappa = \kappa - \kappa_{el}$, (dashed) as a function of T. Selected data near 100 K and 300 K show representative 5% systematic uncertainty, see SM: [14]. Gray bar indicates critical region where the WF law breaks down.

$L_0T/\rho(T)$, also shown in Fig. 4. This allows us to define a "non-electronic" contribution $\Delta\kappa \equiv \kappa - \kappa_{el}$. While it is conventional to identify $\Delta\kappa$ with an independent phonon contribution, $\Delta\kappa \leftrightarrow \kappa_{ph}$, it is apparent (discussed below) this is not plausible over much of the temperature range and especially in a region immediately below T_{CDW1} (gray bar in Fig. 4).

We first consider room temperature thermal conductivity, above the CDW transitions. The value of the total thermal conductivity is very high compared to other chalcogenide-based CDW materials: $\kappa =$ 0.06 W/cm·K for $TaSe_3$ [21], 0.07 W/cm·K for $NbSe_3$ [22], 0.05 W/cm·K for $(TaSe_4)_2I$ [23], 0.1 W/cm·K for 2H-$TaSe_2$ [24], 0.035 W/cm·K for $HfTe_5$ [25], or 0.08 W/cm·K at 370K for 1T-TaS_2 [24]. By contrast, $ErTe_3$ exhibits $\sim$ 0.33 W/cm·K at room temperature, more than 3 and up to 10 times larger thermal conductivity than those compounds. However, using WF law and our measured resistivity to evaluate the electronic thermal conductivity, we obtain a value of $\Delta\kappa$ comparable in magnitude to these materials. Considering the much larger resistivities of these other materials, WF analysis yields a relative κ_{el}/κ of around 20% to 25% for most compounds, reaching 45% for $NbSe_3$ nanowires [22]. In all cases κ is very weakly T dependent in this range of temperature. One naturally identifies $\Delta\kappa \approx \kappa_{ph}$ as an essentially independent phonon contribution to the thermal conductivity - as commonly done.

WF law is expected to work at temperatures comparable and above the Debye temperature (θ_D), relying on quasi-elastic electron-phonon scattering applicable for modes whose characteristic frequencies, $\omega \ll k_BT/\hbar$, and all nearly critical modes due to critical slowing down. Thus, analysis of the CDW transition region, particularly the anomaly at T_{CDW1}, which is $\sim$ 100 K above θ_D, implies a catastrophic breakdown of the WF approach. While based on WF law, one would expect the critical anomaly in the total thermal conductivity to be weak similar to the resistivity, it is in fact pronounced and resembles the behavior of $d\rho/dT$. (Note the relatively weak specific heat anomaly at T_{CDW1}, primarily because the high transition temperature where the specific heat is already in the Dulong-Petit regime). More dramatically, if we use the WF law to subtract an electronic contribution to κ in the critical regime, we would be forced to conclude that the lattice contribution $\Delta\kappa$ mysteriously vanishes, at least within $\sim$ 30 degrees below T_{CDW1} - indicated by the gray bar in Fig. 4. This sharp decrease in $\Delta\kappa$ in $ErTe_3$ and the strong violation of the WF law is quite different from other 1D CDW materials including $Lu_5Ir_4Si_{10}$ [26], $LaAgSb_2$ [27], and CuTe [28], where the WF is followed through T_{CDW} irrespective whether the electrical resistivity changes gradually or sharply. We know of no plausible physical mechanism that could produce such an effect. However, if inelastic scattering of the electrons from the critical modes plays a role in the breakdown of the WF law, this would be highly anomalous and suggests an unexpectedly intimate connection between the electronic and lattice degrees of freedom.

Below $\sim$ 240 K, $\Delta\kappa$ reaches $\sim$ 0.05 W/cm·K, common to this type of materials, and thus again can be loosely interpreted as parallel lattice contribution. Using simple kinetic theory, our measured specific heat, and typical longitudinal sound velocity of $\sim 2.8 \times 10^5$cm/s [10, 19], we obtain a mean free path of $\sim$ 35 Å at $T = T_{CDW2}$, reduced from $\sim$ 80 Å above T_{CDW1}. While below the primary CDW transition the phonon mean free path might be expected to increase reflecting reduced phonon-electron scattering, CDW fluctuations in the transition region, and CDW formation below that temperature could be additional sources of phonon scattering. (By contrast, in other chalcogenide-based CDW materials κ is nearly constant with a slight tendency to increase with decreasing T over the same temperature range.) Over the same temperature range, the total and electronic thermal conductivities reach an anisotropic value of $\kappa^c/\kappa^a \approx \kappa^c_{el}/\kappa^a_e \approx 1.3$, reflecting the effect of the primary CDW transition at T_{CDW1}. Interestingly, this anisotropy is only weakly reduced below the secondary CDW transition at T_{CDW2}, where the primary effect is an increase in all components of thermal transport. While the increase in the putative lattice part below T_{CDW2} could be from further gapping of electronic states that decrease the phonon-electron scattering rate, the electronic increase in thermal conductivity simply reflects the increase of the mean free path of the remaining itinerant electrons. We check this hypothesis by introducing additional electron disorder scattering with a small concentration of intercalated Pd atoms ($\lesssim$ 1%), which does not markedly change the carrier density [6]. See SM for similar response in $\Delta\kappa$ when there is $\sim$ 0.3% Pd intercalation [14].

Figure 3 shows the effect of $\sim 0.3\%$ Pd intercalation on the thermal diffusivity. Notice the decrease in the primary CDW transition that follows the phase diagram in [6]. Focusing on a-axis transport, where disorder shows a strong effect on the electronic structure [7], thermal diffusivity in Fig. 3 did not change much below T_{CDW1}, but the characteristic increase below T_{CDW2} is missing, consistent with the increased scattering observed in resistivity (Fig. 1(b)). While this points to an electronic effect, incomplete gapping of electronic states may also affect phonon-electron scattering [7, 8].

Often, transport properties of metals are successfully understood based on the response of weakly interacting elementary excitations — fermionic-quasiparticles and bosonic phonons. In past decades, various transport regimes in certain "highly correlated" materials have been identified, where the validity of this approach has been questioned. However, it remains highly controversial to what extent conventional quasiparticle ideas can be extended without fundamental changes in approach to strongly interacting regimes where the quasiparticle identity is "marginally" maintained, or if entirely new paradigms (e.g. some form of "non-Fermi liquid" or novel fractionalized quasiparticles) are needed.

One approach to attack this problem has been to investigate the breakdown of quasiparticle picture near a quantum critical point. However, even at classical (finite T) critical points, the existence of non-trivial critical exponents describing behavior in the critical regime provides clear evidence that critical modes themselves cannot have a quasiparticle description. None-the-less, often, where e.g. Fisher-Langer theory gives good account of transport anomalies, a treatment involving well-defined conduction electrons (and, presumably, phonons) weakly scattered by critical modes, implies that the conventional mechanism of transport theory applies even in the critical regime.

The dramatic failure of this approach to adequately describe thermal transport in $ErTe_3$, most dramatically in the ~ 30 K range below T_{CDW1}, may potentially indicate a simpler context to study the quasiparticle paradigm breakdown. The discrepancies in the critical dependences of thermal conductivity and resistivity in this regime imply a complete breakdown of the WF law, the existence of independent electronic quasiparticles and phonon modes, or both. Indeed, the observed behavior may more adequately be described as a strongly coupled electron-phonon critical 'soup.'

CDW formation is a common phenomenon in quasi-low-dimensional materials, arising from a variety of mechanisms. Although thermal transport measurements have not been widely performed for such materials, they exist for many well-known canonical examples, and in no cases has such dramatic violation of the WF law been deduced. This raises associated questions as why the effect should be so pronounced in this particular material system given the ubiquity of CDW compounds (for a recent survey of CDW systems see e.g. [29]). A wider survey of related materials might reveal that this effect is not unique to the rare earth tritellurides, yet for now $ErTe_3$ occupies a unique position among known CDW compounds and presents an entirely new opportunity to explore unconventional transport properties of strongly interacting metals.

We would like to thank Alan Fang for helpful discussions. This work was supported by the Department of Energy, Office of Basic Energy Sciences, under contract no. DE-AC02-76SF00515. The photothermal apparatus was built using a grant from the Gordon and and Betty Moore Foundation through Emergent Phenomena in Quantum Systems Initiative Grant GBMF4529. JAWS was supported in part by an ABB Stanford Graduate Fellowship. AGS was supported in part by an NSF Graduate Research Fellowship (grant number DGE-1656518). MDB acknowledges partial support from the Swiss National Science Foundation under project number P2SKP2_184069, as well as from the Stanford Geballe Laboratory for Advanced Materials (GLAM) Postdoctoral Fellowship program. XRD measurements were preformed at the Stanford Nano Shared Facilities (SNSF), supported by the National Science Foundation under award ECCS-2026822.

[1] R. E. Peierls, *Quantum theory of solids* (Clarendon Press, Oxford, 1955).
[2] H. Fröhlich, On the theory of superconductivity: The one-dimensional case, Proceedings of the Royal Society A **223**, 296 (1954).
[3] F. Pfuner, P. Lerch, J.-H. Chu, H.-H. Kuo, I. R. Fisher, and L. Degiorgi, Temperature dependence of the excitation spectrum in the charge-density-wave $ErTe_3$ and $HoTe_3$ systems, Phys. Rev. B **81**, 195110 (2010).
[4] R. G. Moore, V. Brouet, R. He, D. H. Lu, N. Ru, J.-H. Chu, I. R. Fisher, and Z.-X. Shen, Fermi surface evolution across multiple charge density wave transitions in $ErTe_3$, Phys. Rev. B **81**, 073102 (2010).
[5] B. F. Hu, B. Cheng, R. H. Yuan, T. Dong, A. F. Fang, W. T. Guo, Z. G. Chen, P. Zheng, Y. G. Shi, and N. L. Wang, Optical study of the multiple charge-density-wave transitions in $ErTe_3$, Phys. Rev. B **84**, 155132 (2011).
[6] J. A. W. Straquadine, F. Weber, S. Rosenkranz, A. H. Said, and I. R. Fisher, Suppression of charge density wave order by disorder in Pd-intercalated $ErTe_3$, Phys. Rev. B **99**, 235138 (2019).
[7] A. Fang, J. A. W. Straquadine, I. R. Fisher, S. A. Kivelson, and A. Kapitulnik, Disorder-induced suppression of charge density wave order: Stm study of pd-intercalated $ErTe_3$, Phys. Rev. B **100**, 235446 (2019).
[8] A. Fang, A. G. Singh, J. A. W. Straquadine, I. R. Fisher, S. A. Kivelson, and A. Kapitulnik, Robust superconductivity intertwined with charge density wave and disorder in pd-intercalated $ErTe_3$, Phys. Rev. Res. **2**, 043221

(2020).
[9] M. E. Fisher and J. S. Langer, Resistive anomalies at magnetic critical points, Phys. Rev. Lett. **20**, 665 (1968).
[10] M. Saint-Paul, G. Remenyi, C. Guttin, P. Lejay, and P. Monceau, Thermodynamic and critical properties of the charge density wave system $ErTe_3$, Physica B: Condensed Matter **504**, 39 (2017).
[11] A. A. Sinchenko, P. D. Grigoriev, P. Lejay, and P. Monceau, Spontaneous breaking of isotropy observed in the electronic transport of rare-earth tritellurides, Phys. Rev. Lett. **112**, 036601 (2014).
[12] N. Ru and I. R. Fisher, Thermodynamic and transport properties of YTe_3, $LaTe_3$, and $CeTe_3$, Phys. Rev. B **73**, 033101 (2006).
[13] J. Zhang, E. M. Levenson-Falk, B. J. Ramshaw, D. A. Bonn, R. Liang, W. N. Hardy, S. A. Hartnoll, and A. Kapitulnik, Anomalous thermal diffusivity in underdoped $YBa_2Cu_3O_{6+x}$, Proceedings of the National Academy of Sciences **114**, 5378 (2017).
[14] (Note), See Supplemental Material at [URL will be inserted by publisher].
[15] P. Walmsley and I. R. Fisher, Determination of the resistivity anisotropy of orthorhombic materials via transverse resistivity measurements, Review of Scientific Instruments **88**, 043901 (2017).
[16] N. Ru, C. L. Condron, G. Y. Margulis, K. Y. Shin, J. Laverock, S. B. Dugdale, M. F. Toney, and I. R. Fisher, Effect of chemical pressure on the charge density wave transition in rare-earth tritellurides $R\mathrm{Te}_3$, Phys. Rev. B **77**, 035114 (2008).
[17] J. T. Fanton, D. B. Mitzi, A. Kapitulnik, B. T. Khuri-Yakub, G. S. Kino, D. Gazit, and R. S. Feigelson, Photothermal measurements of high tc superconductors, Applied Physics Letters **55**, 598 (1989), https://doi.org/10.1063/1.101843.
[18] Z. Hua, H. Ban, and D. H. Hurley, The study of frequency-scan photothermal reflectance technique for thermal diffusivity measurement, Review of Scientific Instruments **86**, 054901 (2015), https://doi.org/10.1063/1.4919609.
[19] M. Saint-Paul and P. Monceau, Phenomenological approach of the thermodynamic properties of the charge density wave systems, Philosophical Magazine **0**, 1 (2020).
[20] N. Lazarević, Z. V. Popović, R. Hu, and C. Petrovic, Evidence of coupling between phonons and charge-density waves in $ErTe_3$, Phys. Rev. B **83**, 024302 (2011).
[21] B. Zawilski, R. Littleton IV, N. Lowhorn, and T. Tritt, Observation of a two level thermal conductivity in the low-dimensional materials, Solid State Communications **150**, 1299 (2010).
[22] L. Yang, Y. Tao, J. Liu, C. Liu, Q. Zhang, M. Akter, Y. Zhao, T. T. Xu, Y. Xu, Z. Mao, Y. Chen, and D. Li, Distinct signatures of electron-phonon coupling observed in the lattice thermal conductivity of $NbSe_3$ nanowires, Nano Letters **19**, 415 (2019).
[23] R. S. Kwok and S. E. Brown, Thermal conductivity of the charge-density-wave systems $K_{0.3}MoO_3$ and $(TaSe_4)_2I$ near the peierls transition, Phys. Rev. Lett. **63**, 895 (1989).
[24] M. D. Núñez Regueiro, J. M. Lopez-Castillo, and C. Ayache, Thermal conductivity of 1T-TaS_2 and 2H-$TaSe_2$, Phys. Rev. Lett. **55**, 1931 (1985).
[25] B. M. Zawilski, R. T. Littleton, and T. M. Tritt, Description of the parallel thermal conductance technique for the measurement of the thermal conductivity of small diameter samples, Review of Scientific Instruments **72**, 1770 (2001).
[26] Y.-K. Kuo, C. S. Lue, F. H. Hsu, H. H. Li, and H. D. Yang, Thermal properties of $lu_5ir_4si_{10}$ near the charge-density-wave transition, Phys. Rev. B **64**, 125124 (2001).
[27] C. S. Lue, Y. F. Tao, K. M. Sivakumar, and Y. K. Kuo, Weak charge-density-wave transition in LaAgSb2investigated by transport, thermal, and NMR studies, Journal of Physics: Condensed Matter **19**, 406230 (2007).
[28] C. N. Kuo, R. Y. Huang, Y. K. Kuo, and C. S. Lue, Transport and thermal behavior of the charge density wave phase transition in cute, Phys. Rev. B **102**, 155137 (2020).
[29] M. Saint-Paul and P. Monceau, Survey of the thermodynamic properties of the charge density wave systems, Advances in Condensed Matter Physics **2019**, 2138264 (2019).